24th IMEKO TC4 International Symposium
22nd International Workshop on ADC and DAC Modelling and Testing
IMEKO TC-4 2020
Palermo, Italy, September 14-16, 2020

VNA-based broadband EVM measurement of an RF nonlinear PA under load mismatch conditions

G. P. Gibiino[1], A. M. Angelotti[1], A. Santarelli[1], P. A. Traverso[1]

[1]*Dept. Electrical, Electronic, and Information Engineering (DEI), University of Bologna, Italy*

***Abstract* – In the context of modern communications systems operating at radio-frequency (RF), the error vector magnitude (EVM) is the most commonly adopted metric to quantify modulation distortion caused by a nonlinear device. While EVM is typically measured with instrumentation featuring broad acquisition bandwidth (BW), here we implement a method based on multiple narrowband vector network analyzer (VNA) acquisitions, allowing for improved measurement accuracy and for broader characterization BWs. We report the EVM characterization of a nonlinear RF power amplifier (PA), analyzing, in particular, the case of the PA cascaded with a linear network, under load mismatch conditions as imposed by a narrowband passive tuner.**

I. INTRODUCTION

Modern communications systems working with broadband modulated signals, and in particular 5G systems, are prospected to operate with bandwidths (BWs) up to 100 MHz per channel for frequency range one (FR1) and 400 MHz per channel for frequency range two (FR2) [1], hence with GHz-wide BWs in a multi-channel scenario. At the same time, modulations schemes such as 256-QAM, necessary for high data-rate, can be effectively deployed only if a sufficient dynamic range can be guaranteed across the whole signal chain for both transmitters and receivers.

In this context, the most widely adopted metric to characterize the modulation distortion induced by hardware is the error vector magnitude (EVM) [2]:

$$\mathrm{EVM} = \sqrt{\frac{\sum_{n=1}^{N} |S_n - S_n^r|^2}{\sum_{n=1}^{N} |S_n|^2}} \qquad (1)$$

where S_n^r is the nth received modulation symbol, S_n is the corresponding symbol of the ideal constellation, and N are the symbols considered.

Let us consider the EVM measurement setups in Fig. 1, where the electrical variables at the DUT ports (port 1 and port 2) are conveniently expressed in terms of incident (a) and reflected (b) waves. The standard bench for measuring the EVM, shown in Fig. 1a, features baseband signal generation by an arbitrary waveform generator (AWG), which synthesizes the in-phase and quadrature (IQ) signal components necessary for complex modulation. These are upconverted by an IQ mixer at the radio-frequency (RF) carrier frequency, realizing a Vector Signal Generator (VSG). The incident wave (a_1) is applied to the device-under-test (DUT), whose output wave (b_2) is directly injected into a receiver composed by an IQ mixer for IQ-demodulation, and a digitizer for the actual signal acquisition at baseband. Such a receiver setting is usually implemented in vector signal analyzers (VSAs), along with suitable techniques for recovering the carrier frequency and the signal constellation. Hence, the EVM can be mathematically calculated with (1), comparing the received and equalized symbols (S_n^r) with the reference constellation symbols (S_n).

Despite the research in broadband and high-dynamic-range receivers, guaranteeing a sufficient EVM measurement accuracy for 5G GHz-wide BWs at high carrier frequencies represents a challenging task, and even state-of-the-art VSAs might not be adequate for the purpose. Therefore, new frequency-domain techniques have been recently proposed [3] to more accurately measure the EVM with a setup based on a Vector Network Analyzer (VNA), such as the one reported in Fig. 1b, where the subscript m stands for the quantities actually measured by the VNA

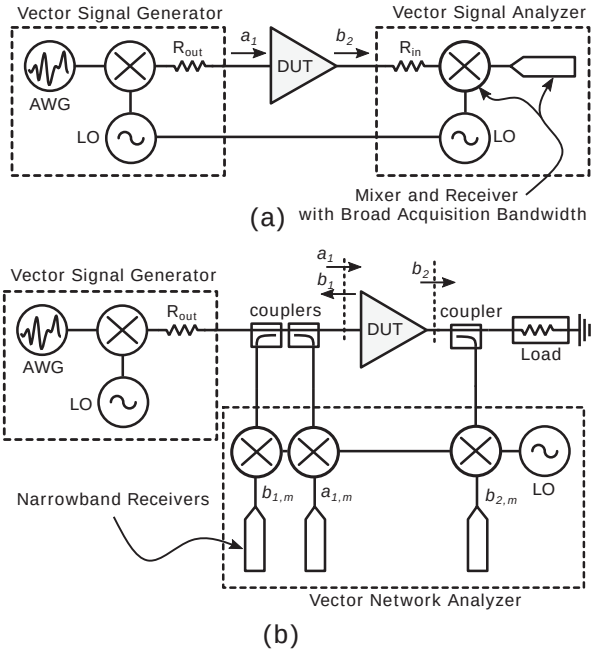

Fig. 1. (a) EVM measurement setup based on a vector signal analyzer. (b) EVM measurement setup based on a vector network analyzer, as addressed in this work.

receivers, i.e., the voltage at the coupled arms of the reflectometers after frequency down-conversion.

These methods stem from the best linear approximation (BLA) framework [4, 5, 6], which allows to de-embed an optimal (in the least-square sense) linear dynamic approximation of the DUT for a given excitation class. EVM then corresponds to the residual uncorrelated nonlinear distortion contribution, closely approximating the EVM value that would be measured after receiver equalization in a classic VSA-based setup [3].

The BLA-based approach requires the synchronous acquisition of calibrated relative measurements of the waves at the DUT ports, as can be easily accomplished by VNA technology. By exploiting periodic multi-tone test signals suitably derived from standard test waveforms [1], these VNA-based techniques avoid phase-coherent IQ frequency down-conversion, removing the demanding instantaneous BW requirement. Instead, they use multiple narrowband acquisitions by sweeping the local oscillator (LO) across the BW like in normal VNA operation, with a clear advantage in terms of reduced measurement noise. Eventually, accurate EVM characterization is enabled across the whole BW of the VNA test-set, which can extend to several tens of GHz.

Taking into account the whole transmitter-receiver chain of a modern telecom system, the power amplifier (PA) used in the final stages of the transmitter is usually the most significant cause of nonlinear distortion. In this respect, it is particularly relevant to evaluate the impact of different PA operating conditions on the EVM degradation.

In this contribution, we review and implement the VNA-based EVM characterization proposed in [6] for an off-the-shelf RF PA. With respect to previous works [3, 6, 7], the implications on the EVM measurement are studied when a nonlinear-dynamic PA under test is cascaded with a linear two-port network. This is a common application example corresponding to the presence of load mismatch due to, for example, a filter, an antenna, or a load-pull testing scenario. In this latter case, the measurement of the EVM at different load mismatch conditions (i.e., in a non-50-Ω environment) has indeed been shown [8] to be a valuable tool for characterizing the intrinsic broadband distortion performance of electron device technologies used in RF PAs at an early stage of testing.

II. MEASUREMENT-BASED EVM MODEL

Using the BLA framework [5], for a generic input spectrum $X(f)$, the output spectrum $Y(f)$ for any nonlinear-dynamic period-preserving system can be expressed as:

$$Y(f) = G_{YX}(f)X(f) + D_{YX}(f) + N_Y(f); \quad (2)$$

where G_{YX} is the least-square best approximation of a linear dynamic frequency response function (FRF) of the system across all the excitations for a given signals' class [5]; $D_{YX}(f)$, a zero-mean contribution with variance $\sigma^2_{D_{YX}}(f)$, quantifies the input-uncorrelated nonlinear stochastic distortions; $N_Y(f)$, with variance $\sigma^2_{N_Y}(f)$, represents additive measurement noise.

Equation 2, corresponding to Fig. 2a, can be seen as a model for the generic VSA-based receiver operation in Fig. 1a, where the linear equalization basically implements the estimation and compensation of G_{YX}. Using (2), the EVM_{YX} results [6]:

$$\text{EVM}_{YX} = \sqrt{\frac{\int_{\text{BW}} \sigma^2_{D_{YX}}(f)df}{\int_{\text{BW}} |G_{YX}(f)|^2 S_{XX}(f)df}} \quad (3)$$

where $S_{XX}(f)$ is the input power spectral density (PSD), the expression $|G_{YX}(f)|^2 S_{XX}(f)$ depicts the linearly input-correlated PSD across the excitation BW, and

$$\sigma^2_{D_{YX}}(f) = S_{YY}(f) - |G_{YX}(f)|^2 S_{XX}(f) \quad (4)$$

is the purely nonlinear distortion power, $S_{YY}(f)$ being the output PSD.

Let us consider a flat-amplitude, periodic random-phase multi-tone input $X(f)$ with a given BW and excitation frequencies f_l, $l = 1, \ldots, L$. With a sufficiently high number of tones, the statistical characteristics of such input signal can closely match any other excitation sharing the same PSD and complex-gaussian envelope probability density function (PDF) [6]. The following FRF at the f_l can be obtained from relative measurements:

$$G^{[r,p]}_{YX}(f_l) = \frac{Y(f_l)^{[r,p]}}{X(f_l)^{[r,p]}}; \quad r = 1, \ldots, R; \quad p = 1, \ldots, P; \quad (5)$$

P being the number of repeated acquisitions for each of R different random-phase realizations of the multi-tone input signal. Averaging $G^{[r,p]}_{YX}$ across the P periods leads to

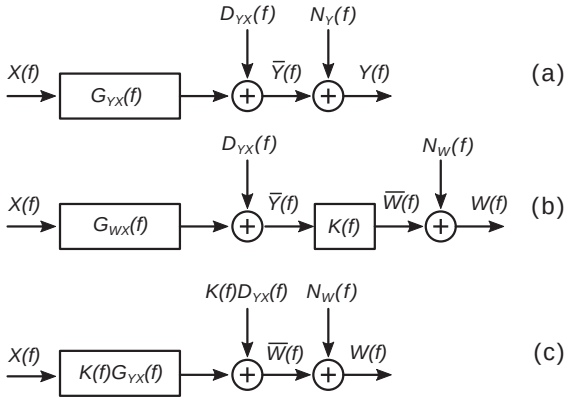

Fig. 2. Measurement-based EVM model. (a) Case for a nonlinear-dynamic system. (b) Case for a nonlinear-dynamic system cascaded with a linear system $K(f)$. (c) Case for a nonlinear-dynamic system corresponding to (b).

an estimation of the noise variance $\sigma^2_{G_N}(f_l)$ of $G_{YX}(f_l)$, while averaging across the R realizations allows to quantify the distortion power $\sigma^2_{G_D}(f_l)$ and the actual value of $G_{YX}(f_l)$ [5]. It can be proved [6] that

$$\sigma^2_{D_{YX}}(f_l) = \sigma^2_{G_D}(f_l) S_{XX}(f_l), \tag{6}$$

so that the EVM in (3) can be eventually calculated, where the integration simplifies to a sum across the f_l frequencies.

Considering the VNA-based setup in Fig. 1b and the frequency domain representation, let us adopt the incident wave at port 1 $A_1(f)$ (in the frequency domain) as the input signal and the reflected wave at port 2 $B_2(f)$ (in the frequency domain) as the output signal. Provided that a relative vector calibration[1] and a receiver power calibration at the DUT reference planes are implemented, the FRF in (5) can be characterized by means of multiple VNA synchronous relative measurements. These experiments actually correspond to performing frequency sweeps across the L excited frequencies akin to the classic measurement of the DUT complex gain. Due the presence of a power calibration, the power-calibrated PSDs $S_{B_2B_2}(f_l)$ and $S_{A_1A_1}(f_l)$ can be straightforwardly acquired. From this experimental data, the value of $\text{EVM}_{B_2A_1}$ can be eventually obtained.

III. EXPERIMENTAL RESULTS

A. Measurement setup

The actual VNA-based measurement setup used in this work is reported in Fig. 3. The DUT is an off-the-shelf PA from Mini-Circuits excited with a 100-MHz-BW, L-tone random phase multitone signal (L =1001) centered at 1.75 GHz. The frequency spacing among the tones is 100 kHz. The signal PDF is gaussian with band-limited white PSD, reproducing a suitable test signal as from the 5G FR1 standard [1]. This input signal is generated by a Keysight MXG N5182B VSG, while the VNA in use is the Keysight PNA-X N5242A. The DUT is cascaded with a manual slide screw tuner (Maury Microwave 7941A), which constitutes a tunable two-port linear network described by the following transfer matrix:

$$\mathbf{T}_{32}(f) = \begin{bmatrix} t^{11}_{32}(f) & t^{12}_{32}(f) \\ t^{21}_{32}(f) & t^{22}_{32}(f) \end{bmatrix}. \tag{7}$$

Three ports and corresponding calibration reference planes are defined, each port using a two directional couplers (or reflectometers) for wave sensing (internal VNA couplers for ports 1 and 3, external couplers for port 2). The first two ports correspond to the input and the output of the PA, while the third one lays after the tuner. The VSG is connected to a rear-panel connector of the VNA and internally re-directed to inject into port 1. A classic three-port short-open-load-thru relative calibration has been performed, as well as a receiver power calibration referenced to a power meter. All six waves at the three ports are measured in the experimental tests.

B. EVM of PA under load mismatch conditions

The cascaded linear two-port network represented by the tuner imposes the reflection coefficient at port 2

$$\Gamma_{L,2}(f) = \frac{A_2(f)}{B_2(f)} \tag{8}$$

and, in general, synthesizes mismatch conditions for the PA. In this context, it is worth analyzing if $\text{EVM}_{B_2A_1}$, i.e., with $B_2(f)$ as output and $A_1(f)$ as input, is an effective metric in representing the modulation distortion of the whole PA-tuner chain. Indeed, it could be argued that the distortion measured on the reflected wave $A_2(f)$ or on the waves at the load reference plane at port 3:

$$\begin{bmatrix} A_3(f) \\ B_3(f) \end{bmatrix} = \mathbf{T}_{23}(f) \begin{bmatrix} A_2(f) \\ B_2(f) \end{bmatrix} \tag{9}$$

could be generally different from the one on $B_2(f)$. In this respect, we will consider the typical case in which

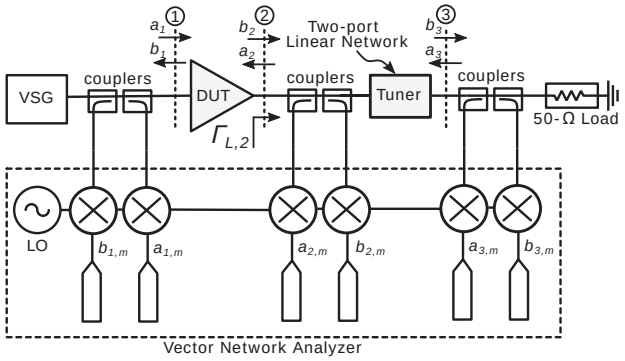

(a)

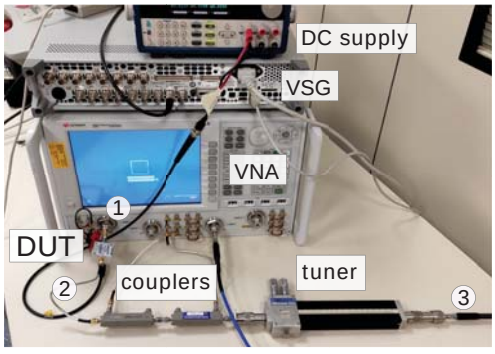

(b)

Fig. 3. Block diagram (a) and photo (b) of the VNA-based measurement setup used for EVM characterization.

[1] b_1 wave sensing in Fig. 1b is necessary for relative calibration [3].

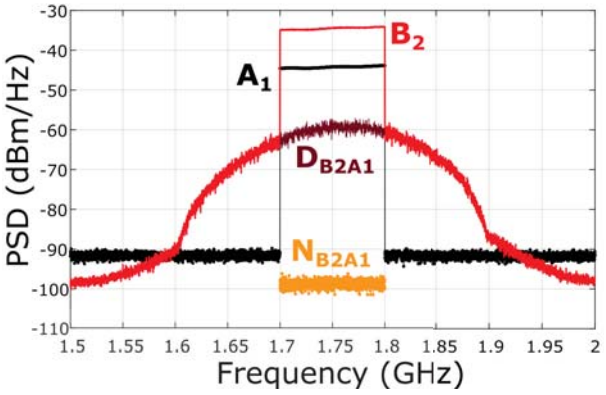

Fig. 4. Frequency spectra of the quantities measured for characterizing EVM$_{B_2A_1}$ ($\Gamma'_{L,2}(f)$ load, $P_{av,s}$=-6.9 dBm).

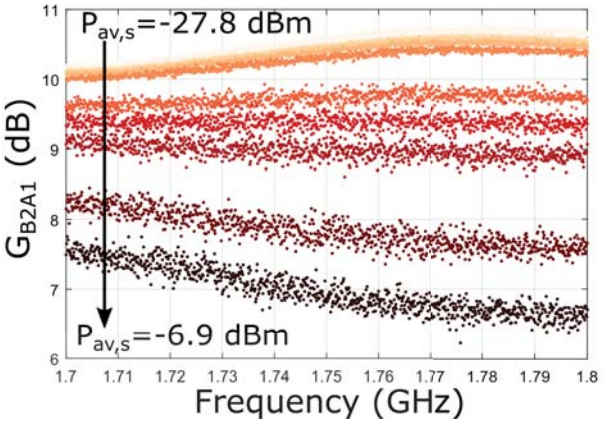

Fig. 5. $G_{B2A1}(f)$ at different $P_{av,s}$ for the $\Gamma'_{L,2}(f)$ load.

$Z_{L,3} = 50\ \Omega$ and $A_3(f) = 0$, with the result that

$$B_3(f) = (t_{32}^{21}(f)\Gamma_{L,2}(f) + t_{32}^{22}(f))B_2(f), \qquad (10)$$

with $A_2(f) = \Gamma_{L,2}(f)B_2(f)$.

The procedure described in Sec. II, with $P = 2$ and $R = 25$ in (5), has been firstly applied for characterizing EVM$_{B_2A_1}$ at different RF available source power ($P_{av,s}$), obtaining the results in Figs. 4-6 for the $\Gamma'_{L,2}$ profile reported in the inset of Fig. 6.

The frequency-domain quantities in Fig. 4 are acquired with VNA frequency sweeps across the 100-MHz BW with receivers intermediate frequency BW of 1 kHz. The in-band distortion $D_{B2A1}(f)$ can be measured with a remarkably low noise level, showing a continuous profile with the out-of-band re-growth [6, 3]. The G_{B2A1} (Fig. 5) depends on the large-signal operating point (hence, on $P_{av,s}$ and load profile). Since $G_{B2A1}(f)$ is identified by averaging out the nonlinear stochastic distortion and that R is fixed for all cases, $G_{B2A1}(f)$ traces show larger spread as $P_{av,s}$ increases: larger values of R would asymptotically result into a continuous $G_{B2A1}(f)$ [3]. The EVM$_{B_2A_1}$ can be accurately measured below 1%, and its trend was characterized up to 10% for the maximum $P_{av,s}$ applied, as shown in Fig. 6.

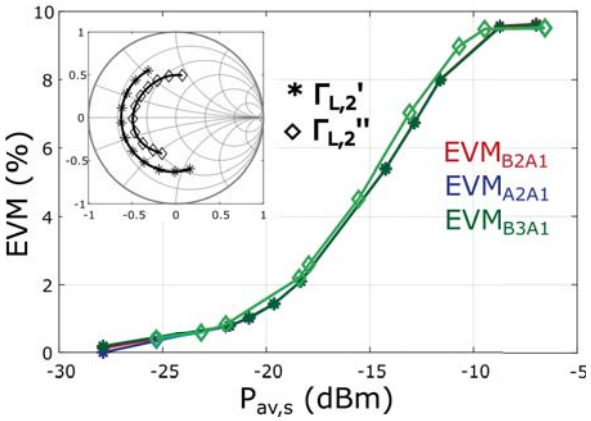

Fig. 6. EVM profile as a function of $P_{av,s}$ for B_2, A_2 and B_3, for the loads $\Gamma'_{L,2}(f)$ and $\Gamma''_{L,2}(f)$.

Then, the procedure has been applied to the case of a nonlinear network cascaded with a linear one, described by $K(f)$ in Fig. 2b, obtaining the two following EVM characterizations, both using $A_1(f)$ as input:

1. EVM$_{A_2A_1}$, where the output $W(f)$ corresponds to $A_2(f)$ and $K(f) = \Gamma_{L,2}(f)$;

2. EVM$_{B_3A_1}$ where the output $W(f)$ corresponds to $B_3(f)$ and $K(f) = t_{32}^{21}(f)\Gamma_{L,2}(f) + t_{32}^{22}(f)$.

The results for two load profiles $\Gamma'_{L,2}(f)$ and $\Gamma''_{L,2}(f)$ are reported in Fig. 6. The three EVM values for a given $\Gamma_{L,2}(f)$ correspond (up to measurement noise), proving that the choice of measurement variable does not impact the actual EVM value. Any of the $B_2(f)$, $A_2(f)$, or $B_3(f)$ can be theoretically used for the characterization, although it is reasonable to choose the one for which the highest acquisition dynamic range can be guaranteed.

Conversely, BLAs differ depending on the output signal, as shown in Fig. 7. In fact, in each case, the BLA accounts for the cascaded linear network, so that the measurement model of Fig. 2b actually corresponds to the general model of a nonlinear-dynamic system (Fig. 2a) with the BLA and the stochastic distortion contribution multiplied by $K(f)$, resulting in Fig. 2c.

When the load is changed, for example synthesizing $\Gamma''_{L,2}(f)$ also shown in the inset of Fig. 6, a different EVM value and corresponding BLAs are measured, as the nonlinear PA will operate at a different large-signal operating point. Nevertheless, also in this second case, the choice of the output variable does not influence the EVM measurement.

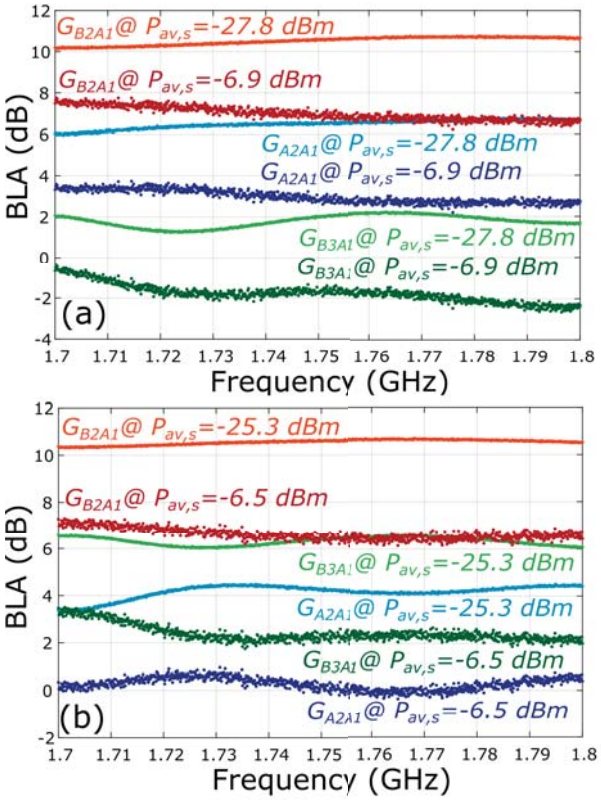

Fig. 7. $G_{B2A1}(f)$, $G_{A2A1}(f)$ *and* $G_{B3A1}(f)$ *at two different* $P_{av,s}$ *for a)* $\Gamma'_{L,2}(f)$ *and b)* $\Gamma''_{L,2}(f)$.

IV. CONCLUSION

This work reports a VNA-based, EVM measurement technique for the characterization of modulation distortion of an RF PAs under load mismatch. Theoretical derivations and experimental evidence prove that the measured EVM value, while generally depending on the load, is the same for all the waves variables of the linear two-port network cascaded with the PA. Thus, differently from other distortion metrics such as Adjacent-Channel Power Ratio (ACPR) and Noise-Power Ratio (NPR), the EVM should be regarded as a network metric depending on the DUT, and not on the signal(s) it is measured on. Future work will involve the VNA-based EVM characterization in the presence of user-imposed broadband load mismatches [9].

ACKNOWLEDGMENT

This work is supported in part by Keysight Technologies, Santa Rosa, California (US).

REFERENCES

[1] *Technical Specification Group Radio Access Network 38.104, 38.141*, 3GPP, 9 2019.

[2] M. D. Mckinley, K. A. Remley, M. Myslinski, J. S. Kenney, D. Schreurs, and B. Nauwelaers, "EVM calculation for broadband modulated signals," in *ARFTG Microwave Measurement Conference*, 2004.

[3] J. Verspecht, A. Stav, J. Teyssier, and S. Kusano, "Characterizing amplifier modulation distortion using a vector network analyzer," in *ARFTG Microwave Measurement Conference*, June 2019, pp. 1–4.

[4] Y. Rolain, W. Van Moer, R. Pintelon, and J. Schoukens, "Experimental characterization of the nonlinear behavior of rf amplifiers," *IEEE Trans. Microw. Theory Techn.*, vol. 54, no. 8, pp. 3209–3218, 2006.

[5] R. Pintelon and J. Schoukens, "FRF measurement of nonlinear systems operating in closed loop," *IEEE Trans. Instrumentation and Measurement*, vol. 62, no. 5, pp. 1334–1345, 2012.

[6] Y. Rolain, M. Zyari, E. Van Nechel, and G. Vandersteen, "A measurement-based error-vector-magnitude model to assess non linearity at the system level," in *IEEE MTT-S International Microwave Symposium*, June 2017, pp. 1429–1432.

[7] A. M. Angelotti, G. P. Gibiino, C. Florian, and A. Santarelli, "Broadband error vector magnitude characterization of a gan power amplifier using a vector network analyzer," in *IEEE MTT-S International Microwave Symposium*, 2020.

[8] M. Marchetti, M. J. Pelk, K. Buisman, W. C. E. Neo, M. Spirito, and L. C. N. de Vreede, "Active harmonic load-pull with realistic wideband communications signals," *IEEE Trans. Microw. Theory Techn.*, vol. 56, no. 12, pp. 2979–2988, Dec 2008.

[9] A. M. Angelotti, G. P. Gibiino, T. S. Nielsen, D. Schreurs, and A. Santarelli, "Enhanced wideband active load-pull with a vector network analyzer using modulated excitations and device output match compensation," in *IEEE MTT-S International Microwave Symposium*, 2020.